Microelectronic Engineering 110 (2013) 40–43

Contents lists available at SciVerse ScienceDirect

Microelectronic Engineering

journal homepage: www.elsevier.com/locate/mee

Investigation of various mechanical bending strains on characteristics of flexible monocrystalline silicon nanomembrane diodes on a plastic substrate

Jung-Hun Seo [b], Yang Zhang [a], Hao-Chih Yuan [b], Yuxin Wang [c], Weidong Zhou [d], Jianguo Ma [a], Zhenqiang Ma [b], Guoxuan Qin [a,*]

[a] School of Electronic Information Engineering, Tianjin University, Tianjin 300072, PR China
[b] Department of Electrical and Computer Engineering, University of Wisconsin-Madison, Madison, WI 53706, USA
[c] Masterwork Machinery Co., Ltd., Tianjin 300400, PR China
[d] Department of Electrical Engineering, NanoFAB Center, University of Texas at Arlington, TX 76019, USA

ARTICLE INFO

Article history:
Received 19 August 2012
Received in revised form 13 April 2013
Accepted 1 May 2013
Available online 9 May 2013

Keywords:
Bending
Diode
Flexible electronic
Microwave
Monocrystalline silicon
Plastic substrate

ABSTRACT

In this paper, comprehensive experimental characterization is conducted for flexible radio frequency (RF) monocrystalline silicon nanomembrane (SiNM) diodes under various bending conditions: convex and concave bendings, paralleled and perpendicular to the diode current flow direction. The flexible diodes indicate significant/slight performance dependence with compressive/tensile bending strains paralleled to or tensile/compressive strains perpendicular to diode current flow direction. Physical and device models are employed to study the underlying mechanism, and demonstrate the dominant changing factor of flexible SiNM diodes under bending conditions. The study provides guidelines for designing and using monocrystalline SiNM diodes for bendable monolithic microwave integrated circuits.

1. Introduction

Flexible electronic devices attract increasing attentions over the past few years, because of their scientific and engineering importance, as well as unique advantages such as bendability, light weight, resistance to impact, conformal attachable to protrusive and irregular shape surfaces, etc. The commonly used materials are organic, polymer, and amorphous/poly-crystalline semiconductor materials [1–5]. However, these materials suffer mainly from their low intrinsic carrier mobility, thus are suitable for low- or modest-speed applications, e.g. imaging/displays, sensors, solar cells, smart cards, etc. [1–5]. Since the realization of transferable monocrystalline silicon nanomembranes (SiNMs), flexible electronics demonstrate great potentials for high speed, high performance applications, ranging from portable wireless devices, long-distance RFIDs, optoelectronics, steerable antennas for communication system, to remote sensing in space and military applications [6–14].

Different from their counterpart of rigid-chip devices, flexible monocrystalline SiNM electronics need to frequently operate under mechanical bending conditions. Therefore it is necessary to conduct thorough investigations on the characteristics of flexible devices under various bending (strain) conditions. Since diode is one of the basic and major components/devices in integrated circuits, we carry out a comprehensive experimental investigation of the various bending effects on flexible monocrystalline SiNM diodes on a plastic substrate (convex and concave bendings, paralleled and perpendicular to the diode current flow direction). Physical and device models are employed to further analyze the underlying mechanism.

2. Experimental results

Fig. 1(a) shows the finished flexible monocrystalline SiNM *p*-type-intrinsic-*n*-type (PIN) diodes on a bent plastic substrate. The diode fabrication is fully compatible with the flexible active component (e.g. thin-film transistor) processes, and the detailed steps can be referred to our previous work [15]. Fig. 1(b) shows the optical-microscope image of a PIN diode with a diode area of 160 μm^2 (two identical p-i-n diode channels, total width is 800 μm), as an example. Fig. 1(c) shows the monocrystalline SiNMs transferred on a PET substrate. Fig. 1(d) shows the cross-section schematic of the device, the intrinsic region length (Li) is ~10 μm. The SiNM is ~200 nm thick. Flexible diode with an area of 320 μm^2 is also used for analysis in this study.

* Corresponding author. Tel./fax: +86 22 27408761.
E-mail address: gqin@tju.edu.cn (G. Qin).

0167-9317/$ - see front matter © 2013 Elsevier B.V. All rights reserved.
http://dx.doi.org/10.1016/j.mee.2013.05.001

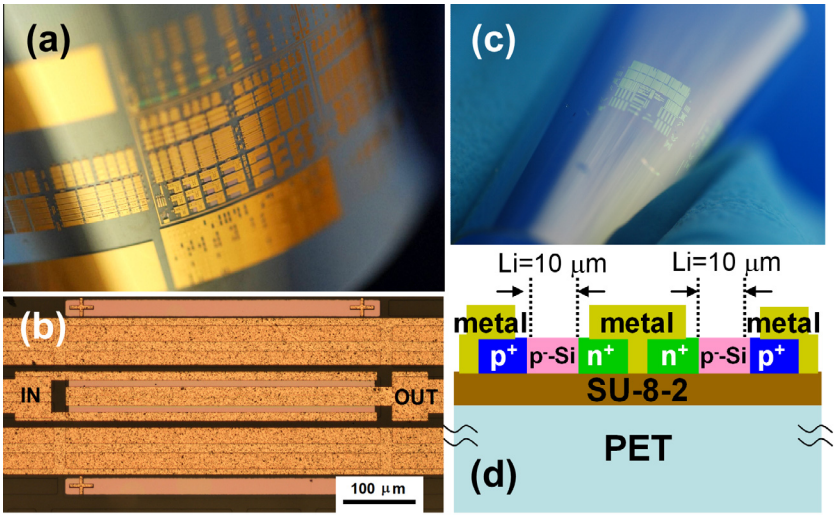

Fig. 1. (a) Optical image of finished flexible monocrystalline SiNM diodes on a bent plastic substrate. (b) Optical-microscope image of a 160 μm^2 flexible PIN diode. The diode has two identical current channels, each with a width of 400 μm. (c) Optical image of transferred monocrystalline SiNM on a plastic substrate. (d) Cross-section schematic of the flexible monocrystalline SiNM diode. Intrinsic region length is ~10 μm.

Ground-signal-ground (GSG) probes and network analyzer (Agilent E8364A) are used to characterize the flexible diodes, and the diode demonstrates high frequency response up to 30 GHz. In addition, the diode indicates better insertion loss while no obvious isolation variation with convex bendings, as shown in Fig. 2. The RF performance dependence of the flexible diodes with convex bendings is consistent with those of diodes with different areas [10]. However, due to the probing limitation of the GSG probes, only convex bending perpendicular to the diode current flow direction is investigated (as illustrated in Fig. 3(a)). Consequently, in order to better understand the strain effects on flexible monocrystalline SiNM devices, as DC probes do not have the probing limitations, we perform comprehensive bending studies on DC characteristics of the monocrystalline SiNM diodes (with an Agilent 4155 semiconductor parameter analyzer). Bending test fixtures with radii ranging from 77.5 to 21 mm (convex) and 110 to 85 mm (concave) are employed. The associated bending tensile strains for the device can be approximately calculated by the following equation: $Strain(\%) = \frac{\Delta R}{2R+\Delta R}$. Where R is the fixture radius (mm), ΔR includes the PET substrate thickness (~175 μm), SU8 layer thickness (~1.8 μm), and the SiNM thickness (~200 nm).

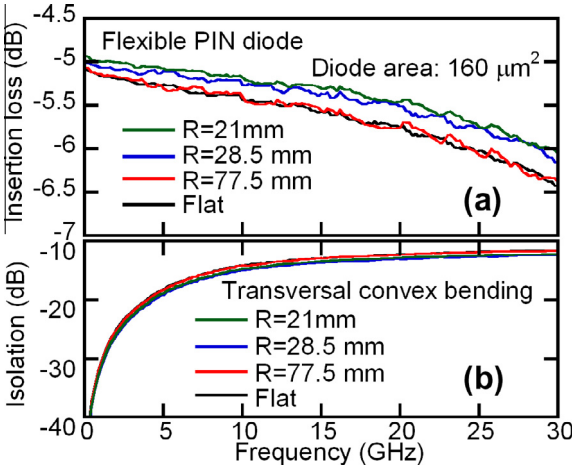

Fig. 2. RF responses of the flexible SiNM diode under transversal convex bending conditions: (a) forward mode insertion loss; (b) reverse mode isolation.

The flexible diodes are first bent along the input-to-output port direction (i.e., perpendicular to diode p-i-n current flow direction, marked as "*T*" for transversal), as illustrated in Fig. 3(a). Fig. 3(b) shows the measured forward I–V properties with various transversal bending radii (bending radius R = 21 mm, 28.5 mm convex bending, and R = 85 mm concave bending, as representative examples). From Fig. 3(b), the flexible monocrystalline SiNM diode shows higher forward current as the transversal convex bending strain becomes larger, and slight current decreasing with concave bending. The diodes are then bent paralleled to the diode current flow direction (marked as "*L*" for longitudinal), as illustrated in Fig. 3(c). Fig. 3(d) shows the measured forward DC properties under various longitudinal bending conditions (R = 21 mm convex bending, and R = 110 and 85 mm concave bending, as representative examples). From Fig. 3(d), the diode shows higher forward current with the longitudinal concave bendings, and decreasing current with convex bending. Flexible diode with an area of 320 μm^2 indicates the same trend (not shown here due to the length limit).

3. Theoretical analysis

In order to have a clear understanding of the relationship between the current changes and various bending directions/strains, it is necessary to examine the flexible diode physical model. The analysis of the current variations under the bending conditions starts from investigation of the forward current which could be described by the thermionic emission theory as shown in Eq. (1) [16]:

$$I = A_{eff} \cdot A^* \cdot T^2 \cdot exp\left(\frac{-q\phi_B}{kT}\right) \cdot exp\left[\frac{-q(V_D - I \cdot R_S)}{nkT}\right] \quad (1)$$

where V_D is the applied voltage, q is the electronic charge, n is the ideality factor, k is the Boltzmann constant, T is the absolute temperature, R_S is the total series resistance (mainly intrinsic region resistance), A_{eff} is the active device area, A^* is the effective Richardson constant (32 A cm^{-2} K^{-2} for silicon) and ϕ_B is the barrier height. According to Eq. (1), at higher voltages, R_S becomes dominant in the diode I–V characteristics. Equation (1) can be rearranged in terms of current density:

$$V_D = R_S \cdot I + n \cdot \phi_B + \left(\frac{nkT}{q}\right) \cdot ln\left(\frac{I}{A_{eff} \cdot A^* \cdot T^2}\right) \quad (2)$$

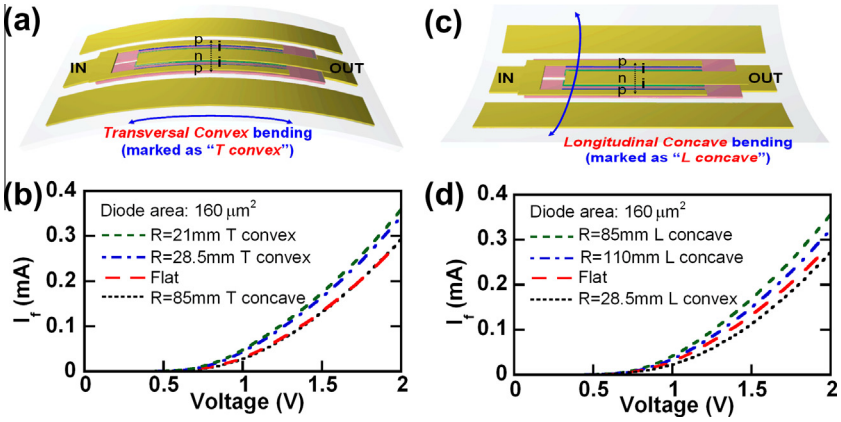

Fig. 3. (a) Schematic of *transversal* (*marked as "T"*) *convex* bending for the diode (i.e., along the input-to-output port direction, or perpendicular to the diode p-i-n current flow direction). (b) Forward I–V characteristics of the flexible monocrystalline SiNM diode under various transversal bending conditions. (c) Schematic of *longitudinal* (*marked as "L"*) *concave* bending for the diode (i.e., paralleled to the diode current flow direction). (d) Forward I–V characteristics of the flexible diode under various longitudinal bending conditions.

To calculate the total series resistance R_S and the ideality factor n, Eq. (2) can be differentiated with respect to the current. By rearranging terms, we obtain $d(V)/d(ln\ I)$ vs. I plot according to Eq. (3).

$$\frac{d(V_D)}{d[ln(I)]} = R_S \cdot I + \frac{nkT}{q} \tag{3}$$

The total series resistance R_S and ideality factor n are calculated from the above expressions. Fig. 4 shows the R_S and n changes by various bending strain conditions. R_S increases from 1.38 to 1.39 kΩ for transversal concave bendings and decreases from 1.38 to 1.32 kΩ for transversal convex bendings. n increases from 1.09 to 1.10 by transversal concave bending while slightly decreases from 1.09 to 1.07 by the transversal convex bending. Opposite result is observed for longitudinal bendings. The R_S and n under longitudinal concave bending decrease from 1.38 to 1.33 kΩ and from 1.09 to 1.07, while they increase from 1.38 to 1.42 kΩ and from 1.09 to 1.13 under longitudinal convex bending, respectively. To further verify the theoretical analysis, I–V characteristics of the flexible monocrystalline SiNM diodes are also investigated employing a PIN diode device model [17]. Fig. 5 (as well as Figs. S2 and S3 in supplementary material) shows good agreement between the model calculation and the experimental results for flexible monocrystalline SiNM diodes with bending strain. According to the device model parameters, total diode series resistance is verified to be the dominant factor and has consistent changing trends with various bending conditions.

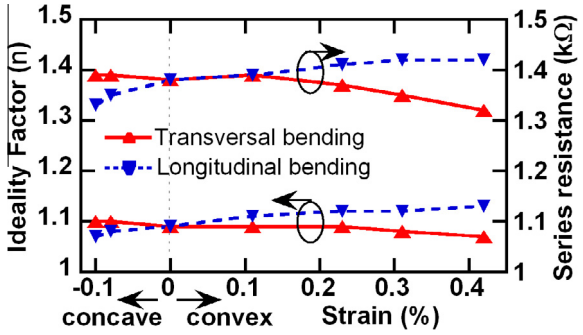

Fig. 4. Total series resistance R_S and ideality factor n of the flexible diode under various bending conditions, calculated from the physical model.

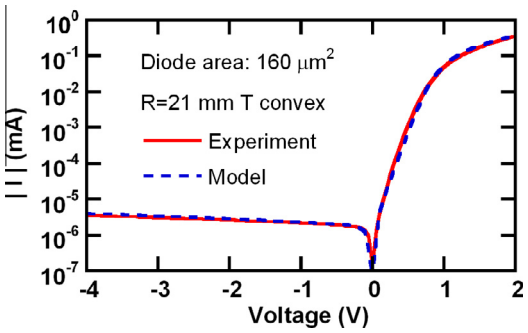

Fig. 5. Comparison of measured (solid lines) and device model calculated (dashed lines) characteristics of the flexible diode under $R = 21$ mm transversal convex bending condition, as an example.

4. Discussion

With the physical model and theoretical calculation, we can better understand the strain effects. From Fig. 3(d), longitudinal concave bending indicates significant influence on the characteristics of flexible monocrystalline SiNM diodes. The major reason is that longitudinal concave bending induces compressive strain paralleled to the current flow direction, resulting in enhancement of the hole mobility [18,19], as the I-region of the diodes is lightly *p*-type doped in this study, the total series resistance R_S (mainly intrinsic region resistance) is reduced (as seen in Fig. 4). And this continues as the strain increases. On the other hand, longitudinal convex bending induces tensile strain to the channel, thus leading to opposite impact. However, since the I-region is lightly *p*-type doped, the tensile strain effect is much smaller [18,19]. This is well verified by the physical model calculations: R_S changes 3.6% for longitudinal concave bending, while changes only 0.72% for longitudinal convex bending of same strain level (as seen from Fig. 4). Fig. 3(b) shows that transversal convex bending also increases the diode forward current. This is because that in-plain tensile strain is applied to the direction perpendicular to the diode current flow direction, and also creates out-of-plain compressive strain due to the Poisson-effect along the current flow direction [20], leading to smaller R_S. The result shows consistency with the RF performance dependence in Fig. 2 (since insertion loss becomes smaller as R_S decreases), as well as flexible microwave diodes with different areas [10,21].

Furthermore, the results indicate that, when the intrinsic region is lightly *p*-type doped (in this study), longitudinal compressive strain has larger effects than transversal tensile strain (as shown in Fig. 3). To be specific, although transversal tensile strain (0.42%, convex bending radius $R = 21$ mm) is much larger than longitudinal compressive strain (0.10%, concave bending radius $R = 85$ mm) in Fig. 3, their influences on the diode characteristics are similar. This can be explained by the theory that the degree of mobility change is varied by the bending directions which tends to increase more under longitudinal strain than transversal strain, due to the different deformation of Δ and L valley of Si band structure [22]. It also agrees well with the theoretical R_S calculations in Fig. 4 (i.e., R_S and n are almost same for longitudinal 0.1% concave bending and transversal 0.42% convex bending cases). According to the analysis, it is also predicted that, if the intrinsic region is lightly *n*-type doped, tensile strain paralleled to the diode current flow direction will have more influence on the characteristics of flexible SiNM diodes.

5. Conclusion

In summary, a comprehensive study is conducted on characteristics of flexible RF monocrystalline silicon nanomembrane (SiNM) diodes under various bending conditions in this letter. The flexible PIN diodes indicate significant/slight performance dependence with compressive/tensile bending strains paralleled to or tensile/compressive strains perpendicular to current flow direction. When the intrinsic region is lightly *p*-type doped, the compressive bending strain paralleled to the diode current flow direction has larger influence on the diode performance than tensile strain perpendicular to the current flow direction. Physical and device model are employed for theoretical analysis and demonstrate that total series resistance is dominant factor for the flexible diode performance change under various bending conditions. The study provides guidelines for designing and using monocrystalline SiNM devices and circuits under mechanical bending conditions.

Acknowledgments

This work was supported by AFOSR under Grant No. FA9550-06-1-0487. This work was also supported by the National Natural Science Foundation of China (NSFC) under Grant No. 61006061, the Tianjin Natural Science Foundation, the Program for New Century Excellent Talents in University (NCET), and the Scientific Research Foundation for the Returned Overseas Chinese Scholars, State Education Ministry.

Appendix A. Supplementary data

Supplementary data associated with this article can be found, in the online version, at http://dx.doi.org/10.1016/j.mee.2013.05.001.

References

[1] H. Sirringhaus, T. Kawase, R.H. Friend, T. Shimoda, M. Inbasekaran, W. Wu, E.P. Woo, Science 290 (2000) 2123.
[2] Y. Chen, J. Au, P. Kazlas, A. Ritenour, H. Gate, M. McCreary, Nature 423 (2003) 136.
[3] T. Takenobu, N. Miura, S.-Y. Lu, H. Okimoto, T. Asano, M. Shiraishi, Y. Iwasa, Applied Physics Express 2 (2009) 025005.
[4] G. Qin, H.-C. Yuan, H. Yang, W. Zhou, Z. Ma, Semiconductor Science and Technology 26 (2011) 025005.
[5] J.-H. Kwon, S.-I. Shin, K.-H. Kim, M. Cho, K. Kim, D. Choi, B.-K. Ju, Applied Physics Letters 94 (2009) 013506.
[6] E. Menard, K.J. Lee, D.-Y. Khang, R.G. Nuzzo, J.A. Rogers, Applied Physics Letters 84 (2004) 5398.
[7] J.A. Rogers, M.G. Lagally, R.G. Nuzzo, Nature 477 (2011) 45.
[8] R.H. Reuss, B.R. Chalamala, A. Moussessian, M.G. Kane, A. Kumar, D.C. Zhang, J.A. Rogers, M. Hatalis, D. Temple, G. Moddel, B.J. Eliasson, M.J. Estes, J. Kunze, E.S. Handy, E.S. Harmon, D.B. Salzman, J.M. Woodall, M.A. Alam, J.Y. Murthy, S.C. Jacobsen, M. Olivier, D. Markus, P.M. Campbell, E. Snow, Proceedings of IEEE 93 (2005) 1239.
[9] Z. Ma, Science 333 (2011) 830.
[10] G. Qin, H.-C. Yuan, G.K. Celler, J. Ma, Z. Ma, Applied Physics Letters 97 (2010) 233110.
[11] G. Qin, H.-C. Yuan, Y. Qin, J.-H. Seo, Y. Wang, J. Ma, Z. Ma, IEEE Electron Device Letters 34 (2013) 160.
[12] J.H. Ahn, H.S. Kim, K.J. Lee, Z.T. Zhu, E. Menard, R.G. Nuzzo, J.A. Rogers, IEEE Electron Device Letters 27 (2006) 460.
[13] G. Qin, J.-H. Seo, Y. Zhang, H. Zhou, W. Zhou, Y. Wang, J. Ma, Z. Ma, IEEE Electron Device Letters 34 (2013) 262.
[14] L. Sun, G. Qin, J. Seo, G.K. Celler, W. Zhou, Z. Ma, Small 6 (2010) 2553.
[15] G. Qin, H.-C. Yuan, G.K. Celler, W. Zhou, J. Ma, Z. Ma, Microelectronics Journal 42 (2011) 509.
[16] S.K. Cheung, N.W. Cheung, Applied Physics Letters 49 (1986) 85.
[17] S.M. Sze, Physics of Semiconductor Devices, 2nd ed., Wiley & Sons, New York, 1981. Chap. 2.
[18] S. Suthram, J.C. Ziegert, T. Nishida, S.E. Thompson, IEEE Electron Device Letters 28 (2007) 58.
[19] W. Zhao, J. He, R.E. Belford, L.-E. Wernersson, A. Seabaugh, IEEE Transactions on Electron Devices 51 (2004) 317.
[20] Y. Sun, S.E. Thompson, T. Nishida, Journal of Applied Physics 101 (2007) 104503.
[21] G. Qin, L. Yang, J.-H. Seo, H.-C. Yuan, G.K. Celler, J. Ma, Z. Ma, Applied Physics Letters 99 (2011) 243104.
[22] F. Chen, C. Euaruksakul, Z. Liu, F.J. Himpsel, F. Liu, M.G. Lagally, Journal of Physics D: Applied Physics 44 (2011) 325107.